

A titanium-nitride near-infrared kinetic inductance photon-counting detector and its anomalous electrodynamics

J. Gao, M. R. Vissers, M. O. Sandberg, F. C. S. da Silva, S. W. Nam, D. P. Pappas, D. S. Wisbey, E. C. Langman, S. R. Meeker, B. A. Mazin, H. G. Leduc, J. Zmuidzinas, and K. D. Irwin

Citation: *Applied Physics Letters* **101**, 142602 (2012); doi: 10.1063/1.4756916

View online: <http://dx.doi.org/10.1063/1.4756916>

View Table of Contents: <http://scitation.aip.org/content/aip/journal/apl/101/14?ver=pdfcov>

Published by the [AIP Publishing](#)

Articles you may be interested in

[NbTiN superconducting nanowire detectors for visible and telecom wavelengths single photon counting on Si₃N₄ photonic circuits](#)

Appl. Phys. Lett. **102**, 051101 (2013); 10.1063/1.4788931

[Readout-power heating and hysteretic switching between thermal quasiparticle states in kinetic inductance detectors](#)

J. Appl. Phys. **108**, 114504 (2010); 10.1063/1.3517152

[Titanium nitride films for ultrasensitive microresonator detectors](#)

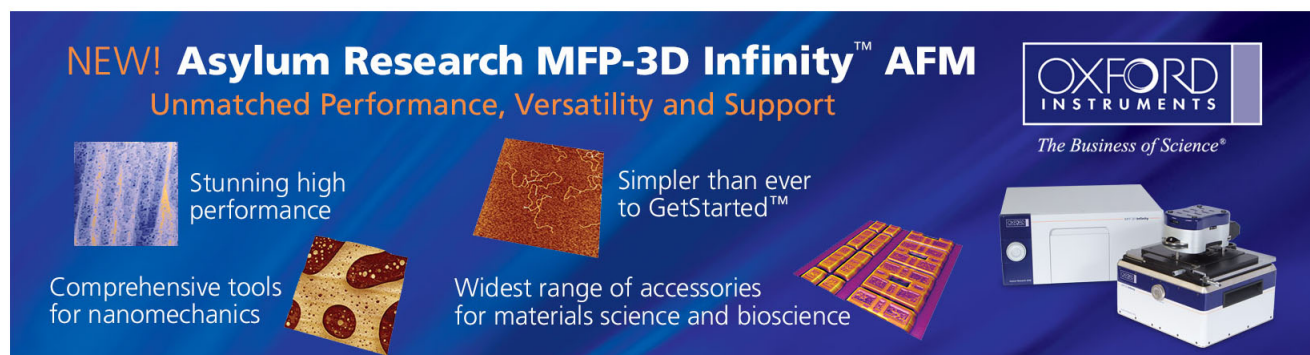
Appl. Phys. Lett. **97**, 102509 (2010); 10.1063/1.3480420

[High-speed phonon imaging using frequency-multiplexed kinetic inductance detectors](#)

Appl. Phys. Lett. **96**, 263511 (2010); 10.1063/1.3459142

[Ultrasensitive hot-electron kinetic-inductance detectors operating well below the superconducting transition](#)

Appl. Phys. Lett. **80**, 817 (2002); 10.1063/1.1445462

The advertisement features a dark blue background with white and orange text. At the top left, it reads 'NEW! Asylum Research MFP-3D Infinity™ AFM' in large white letters, followed by 'Unmatched Performance, Versatility and Support' in orange. On the right, the Oxford Instruments logo is shown with the tagline 'The Business of Science®'. Below the text are four images: a blue textured surface, a brown textured surface, a grid of colorful squares, and a photograph of the MFP-3D Infinity AFM instrument. Text boxes describe the images: 'Stunning high performance' (blue surface), 'Simpler than ever to GetStarted™' (brown surface), 'Comprehensive tools for nanomechanics' (grid of squares), and 'Widest range of accessories for materials science and bioscience' (grid of squares).

A titanium-nitride near-infrared kinetic inductance photon-counting detector and its anomalous electrodynamics

J. Gao,¹ M. R. Vissers,¹ M. O. Sandberg,¹ F. C. S. da Silva,¹ S. W. Nam,¹ D. P. Pappas,¹ D. S. Wisbey,² E. C. Langman,³ S. R. Meeker,³ B. A. Mazin,³ H. G. Leduc,⁴ J. Zmuidzinas,⁴ and K. D. Irwin¹

¹National Institute of Standards and Technology, Boulder, Colorado 80305, USA

²Department of Physics, Saint Louis University, St. Louis, Missouri 63103, USA

³Department of Physics, University of California at Santa Barbara, Santa Barbara, California 93106, USA

⁴Jet Propulsion Laboratory, California Institute of Technology, Pasadena, California 91109, USA

(Received 3 August 2012; accepted 17 September 2012; published online 5 October 2012)

We demonstrate single-photon counting at 1550 nm with titanium-nitride (TiN) microwave kinetic inductance detectors. Full-width-at-half-maximum energy resolution of 0.4 eV is achieved. 0-, 1-, 2-photon events are resolved and shown to follow Poisson statistics. We find that the temperature-dependent frequency shift deviates from the Mattis-Bardeen theory, and the dissipation response shows a shorter decay time than the frequency response at low temperatures. We suggest that the observed anomalous electrodynamics may be related to quasiparticle traps or subgap states in the disordered TiN films. Finally, the electron density-of-states is derived from the pulse response. © 2012 American Institute of Physics. [<http://dx.doi.org/10.1063/1.4756916>]

Fast and efficient photon-counting detectors at near-infrared wavelengths are in high demand for advanced quantum-optics applications such as quantum key distribution^{1,2} and linear-optics quantum computing.³ Superconducting detectors, including superconducting nanowire detectors⁴ and transition-edge sensors (TES),⁵ show great promise in these applications. For example, TES made from tungsten films have shown over 95% of quantum efficiency and photon-number resolving power at 1550 nm.⁶ On the other hand, microwave kinetic inductance detectors (MKIDs) have quickly developed into another major superconducting detector technology for astronomical instruments from submillimeter to x-ray.^{7,8} The main advantages of MKIDs are that they are simple to fabricate and easy to multiplex into a large detector array. Recently, ARCONS or the ARray Camera for Optical to Near-IR Spectrophotometry,⁹ a MKID array made from titanium nitride (TiN) films developed for optical and near-infrared imaging and spectroscopy,¹⁰ has been demonstrated at the Palomar 200-in. telescope. These TiN MKIDs have already shown good photon-counting and energy-resolving capability, but so far they have been considered only for astronomy applications. In this letter, we describe a single-photon-counting experiment at 1550 nm with TiN MKIDs and discuss their promise for application in quantum optics. Another motivation for the work in this letter is to use these detectors to study the electrodynamics and microwave properties of TiN, which is a promising material for MKIDs. Anomalous electrodynamics of TiN is discussed and the density of states $N_0 = 3.9 \times 10^{10} \text{ eV}^{-1} \mu\text{m}^{-3}$ is derived.

MKIDs are thin-film, high-Q superconducting microresonators whose resonance frequency f_r and internal quality factor Q_i (or internal dissipation) change when incoming radiation with photon energy above twice the gap energy ($h\nu > 2\Delta$) breaks Cooper pairs in the superconductor.⁷ The measurements of frequency shift and internal dissipation signals are referred to as frequency readout and dissipation readout, respectively. The principle of operation of the

MKID, as well as the readout schemes, was explained in detail in a recent review paper.¹¹

A recent breakthrough in MKID development is the application of TiN, a superconducting material that shows a number of ideal properties for MKIDs.¹² TiN films have large normal resistivity, high kinetic inductance, and low loss. Resonators made from stoichiometric TiN films (with critical temperature $T_c \sim 4.5 \text{ K}$) have shown $Q_i > 10^6$.¹²⁻¹⁴ In addition, T_c of sub-stoichiometric TiN films can be adjusted between 0 and 4.5 K by varying the nitrogen concentration during deposition. This tuning allows the gap energy and recombination time to be engineered for a specific application. A lower T_c is desired for photon-counting MKIDs, because the detector responsivity in terms of the frequency shift per incident photon scales as $1/\Delta^2$.¹¹

The device used in this work is made from a 20 nm TiN film with $T_c \sim 1 \text{ K}$ deposited on a high-resistivity Si wafer ($>10 \text{ k}\Omega \cdot \text{cm}$). The detector design is adapted from the optical lumped-element (OLE) MKID design used in the ARCONS array¹⁰ and is illustrated in the inset of Fig. 1. The inductive part of the resonator, where photons are absorbed and detected, has been specially tapered to give a uniform current distribution and position-independent response. Resonators with design frequency between 4 and 7 GHz are placed directly next to the center strip of a coplanar waveguide (CPW) feedline (without the ground strip in between) to achieve coupling $Q_c \sim 10\,000$.

The detector wafer was initially etched by use of Cl-chemistry and showed unexpected high level of frequency noise. It was then re-etched briefly for 3 s in SF₆-chemistry to clean off the surface residue left by Cl-etch that was recently found to significantly increase the loss and noise in TiN resonators.¹⁵ The detectors are cooled in an adiabatic demagnetization refrigerator (ADR) to 100 mK and measured in the standard MKID readout (homodyne) scheme with a high electron mobility transistor (HEMT) amplifier (noise temperature $T_n \sim 4 \text{ K}$). A single-mode fiber going into the

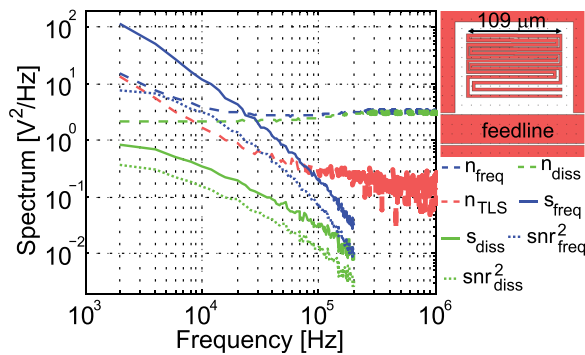


FIG. 1. Spectra of the signal (solid lines), noise (dashed lines), and the signal-to-noise ratio (SNR, dotted lines) in the frequency quadrature (blue) and dissipation quadrature (green) measured at 100 mK. The two-level-system (TLS) noise (red) is inferred from the difference of the noise in the two quadratures. The resonator shows $f_r = 5.8$ GHz and $Q \sim 13$ 000 (internal $Q_i \sim 100$ 000). We use a readout power $P_{\text{feedline}} \approx -95$ dBm that is 1 dB below resonator saturation (bifurcation). Inset: the optical lumped-element (OLE) MKID design.

device box is used to illuminate the entire chip. Outside the ADR, we use a 1550 nm laser diode driven by a function generator to generate optical pulses with width of 200 ns at a repetition rate of 1 kHz. The pulse response signal of the MKID is projected into the frequency and dissipation quadratures, digitized at a sampling rate of 2.5 Ms/s, and processed using a standard Wiener optimal filter, to produce photon-counting statistics.

The detector responses in the frequency quadrature and in the dissipation quadrature measured at 100 mK and averaged over 10 000 optical pulses are shown in Fig. 3(a). The pulse (peak) height is about 5 times larger in the frequency quadrature than in the dissipation quadrature, and interestingly, we also see two different pulse decay times, 65 μ s for the frequency quadrature and 7 μ s for the dissipation quadrature. This anomalous quadrature-dependent response time is discussed below. On the other hand, the measured noise spectra (see Fig. 1) is consistent with the two-level system (TLS) noise picture:¹⁶ there is $1/f$ excess noise below 10 kHz

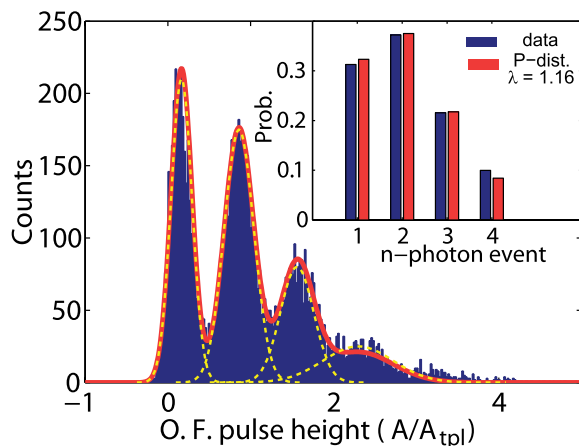


FIG. 2. A histogram of the optimally filtered pulse height (normalized by the template pulse) using the frequency readout. A 4-peak Gaussian fit to the data is shown by the yellow dashed lines, where the 4 peaks from the fitting result are indicated individually. Inset: the area in each Gaussian peak normalized by the total area (blue) fits to a Poisson distribution with $\lambda = 1.16$ (red). The red curve in the main figure shows a convolved profile of the Poisson distribution with $\lambda = 1.16$ and the 4 Gaussians.

in the frequency quadrature and no excess noise above the HEMT noise floor in the dissipation quadrature. The signal and noise spectra shown in Fig. 1 are used to create the optimal filter. Due to the reduced pulse height and shorter response time, the dissipation readout, although free of excess TLS noise, yields a signal-to-noise ratio (SNR) lower by a factor of ~ 4 than the frequency readout. Therefore, we used frequency readout for photon counting experiments.

Fig. 2 shows a histogram of the optimally filtered pulse height using frequency readout. The first 3 peaks are clearly resolved and correspond to the events of 0, 1, and 2 photons being absorbed in the detector. We fit the histogram to a model with a superposition of 4 Gaussian peaks, indicated by the yellow dashed lines in Fig. 2. The full-width-at-half-maximum (FWHM) widths of the first 3 Gaussians (uncertainty is large on the 3-photon peak) correspond to the energy resolutions of $\Delta E = 0.27$ eV, 0.40 eV, and 0.44 eV, respectively. The baseline, $\Delta E = 0.27$ eV, agrees with a SNR analysis from the signal and noise spectra in Fig. 1. We conclude from the 1-photon peak that our TiN photon counting detector has achieved an energy resolution of $\Delta E = 0.4$ eV, corresponding to an energy-resolving power of $R = E/\Delta E = 2$ at 1550 nm, which is consistent with the energy resolution of TiN MKID demonstrated at UV/optical wavelengths¹⁰ and comparable with the energy resolution of

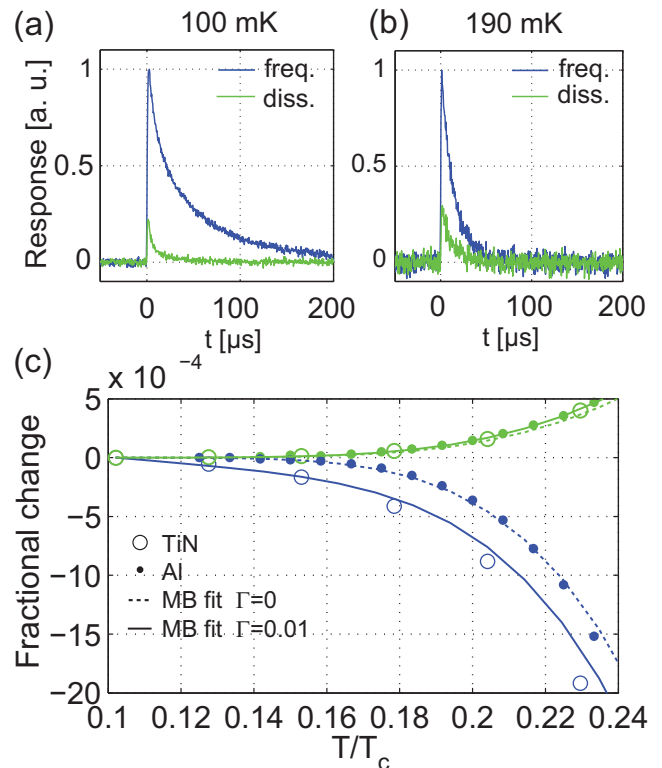


FIG. 3. Anomalous response of TiN MKID. (a) Pulse response at 100 mK. (b) Pulse response at 190 mK. (c) Temperature-dependent frequency response $\frac{\delta f(T)/f_0}{\delta T}$ and dissipation response $\frac{\delta 1/2Q(T)}{\delta T}$ measured for 20 nm TiN ($T_c = 1$ K, $\alpha = 1$, $\gamma = 1$) as compared to 200 nm Al ($T_c = 1.2$ K, $\alpha = 0.276$, $\gamma = 1/3$). α is the measured kinetic inductance fraction²⁴ and γ is a film-dependent index that takes values of 1 in the thin-film limit and 1/3 in the extreme-anomalous limit.²⁵ Fits using Mattis-Bardeen formula with $\Gamma = 0$ and $\Gamma = 0.01$ are indicated by the dotted lines and solid lines, respectively. In (a) and (b), the pulse responses in the two quadratures are normalized by the peak frequency responses. In all the plots, frequency responses are presented in blue and dissipation responses are in green.

a TES detector operating at the same wavelength.⁶ We have also derived an arrival-time resolution of $\Delta t = 1.2 \mu\text{s}$ from the statistics of the arrival time of the optimally filtered pulses.

It is expected from the stochastic nature of the photon detection process that the n -photon events should obey Poisson statistics. Indeed, the counts in the n -photon peak (proportional to and calculated by the area of each Gaussian) normalized by the total counts match a Poisson distribution with $\lambda = 1.16$, as shown in the inset of Fig. 2. In other words, our detector detects an average of 1.16 photons per laser pulsing event in this experiment.

The two different pulse decay times at 100 mK suggest interesting electrodynamic of TiN. We carry out further investigations by repeating the photon counting experiment at elevated bath temperatures between 100 mK and 190 mK. As we raise the bath temperature, we find that the pulse decay time decreases in the frequency response and increases in the dissipation response. At 190 mK, the two quadratures show the same decay times of $16 \mu\text{s}$, as shown in Fig. 3(b). To explain this phenomenon, we propose a hypothesis that low-energy non-dissipative excitation states exist in TiN that give only a reactive response but no dissipative response. At lower temperature (100 mK), the non-dissipative excitation states are mostly vacant. The photon-generated high-energy quasiparticles (QPs) quickly (within $7 \mu\text{s}$) fall into these non-dissipative states and then recombine slowly (within $65 \mu\text{s}$) into Cooper-pairs, leading to an anomalous response with different decay times for the two quadratures. At higher temperature (190 mK), the non-dissipative states are mostly filled up by thermal excitations. The high energy QPs directly combine outside these non-dissipative states, giving a normal response with the same decay time for the two quadratures.¹⁷ One of the physical candidates for the non-dissipative excitation states is quasiparticle traps. TiN films are known to be highly disordered, with localized superconductivity and spatial fluctuations of the gap parameter.¹⁸ In particular, our sub-stoichiometric TiN with $T_c \sim 1 \text{ K}$ sits at a point where T_c is most sensitive to the N_2 concentration.¹² As a result, we find from DC measurement that T_c is highly non-uniform and varies from 0.4 K to 1.3 K over the entire wafer. It is possible that a locally depressed gap can form a potential well and trap a QP.¹⁸ On one hand, because QPs in the traps are frozen in motion, they do not absorb microwave and can be dissipationless. On the other hand, these QPs are removed (excited) from the Cooper-pair condensate and still contribute to a change in the penetration depth. This is because, for example, the penetration depth is related to the density of superconducting electrons by $\lambda_L \propto 1/\sqrt{n_s}$ in the London theory.¹⁹

The hypothesis of non-dissipative excitation states in TiN is further supported by the temperature-dependent frequency shift and dissipation data that also show anomalous feature (Fig. 3(c)). Compared to Al resonators, the TiN resonator shows excess frequency shift seen as an initial slope in $\delta f(T)$ at low temperatures, which deviates from the prediction of the Mattis-Bardeen's formula. This feature has been reported and discussed previously in NbTiN resonators²⁰ (and recently in TiN resonators²¹), where a modified Mattis-Bardeen's formula with a gap-broadening parameter Γ (Dynes parameter²²) was

able to fit the data in Ref. 20. In our case, $\Gamma/\Delta = 0.01$ generates a reasonable fit to the data. Further investigation shows that the density of excitation states modified to include the Dynes' parameter has actually introduced sub-gap states near the Fermi level, which play an important role. Excitations to these sub-gap states at $T < \Delta/k$, which was originally forbidden, give rise to the low-temperature slope in $\delta f(T)$. Interestingly, in this model, these sub-gap states also give a much reduced dissipation response. For example, the real part of the complex conductivity $\sigma_1(T)$ calculated from a QP density of states with/without the Dynes' parameter, or with a wide range of Γ (as long as $\Gamma/\Delta \ll 1$) shows little difference. Therefore, sub-gap states are another physical candidate for the hypothesis of non-dissipative excitation states, and the anomalous temperature and pulse response are consistent under this hypothesis. In fact, sub-gap states deduced from tunneling experiments have been reported for TiN films.²³

Despite the anomalous response at lower temperatures, we use the pulse response at 190 mK to estimate the single-spin electron density of states, N_0 , of TiN. This is one of the most important material parameters for MKID design. From the measured average pulse response of $\delta f_r/f_r = 5.6 \times 10^{-6}$ and the average photon energy of $E = \lambda h\nu$, we have derived

$$N_0 = \frac{\eta E S_2}{4\alpha\gamma\Delta^2 V_{sc} \delta f_r/f_r} = 3.9 \times 10^{10} \text{ eV}^{-1} \mu\text{m}^{-3}, \quad (1)$$

where η is the photon-to-QP conversion factor, commonly assumed to be 0.6, $V_{sc} \approx 70 \mu\text{m}^3$ is the volume of the inductive part of the resonator, and S_2 is the Mattis-Bardeen factor.¹¹ This value of N_0 is about a factor of 4 larger than the theoretical value previously reported.¹²

Our experiment is meant to be a quick demonstration and evaluation of TiN MKIDs for use in quantum optics applications. Many aspects in the experimental configuration and data analysis can be improved. For example, in our current configuration, photons are hitting all parts of the resonator without restriction. This may explain the small positive shift of the 0-photon peak seen in Fig. 2 and may also contribute to the degradation of energy resolution from the baseline resolution. This can be improved by using a focusing lens or a mask to restrict the light to illuminate only the inductive part of the resonator. Also, no attempt has been made in the current device to improve the optical coupling or the quantum efficiency. In addition to using an antireflection-coating, fabricating the long inductive strip of the MKID on top of an optical wave-guide all on a Si wafer might be an interesting scheme to achieve high coupling efficiency. Our TiN MKID has achieved an energy resolution comparable with that of a TES but is much slower.⁶ To further improve the energy resolution or speed up the detector, a lower-noise amplifier (such as the quantum-limited amplifiers currently under development^{26,27}) is probably required. This is because the detector noise is already limited by the HEMT noise in both quadratures at the main Fourier component of the pulse ($\sim 10 \text{ kHz}$), as can be seen in Fig. 1.

We thank T. Klapwijk, T. Norguchi, J. Martinis, G. O'Neill, and A. Lita for useful discussions. We acknowledge support for this work from the Keck Institute for Space

Studies and NASA under Contract No. NNH11AR83I. The TiN film was deposited in the JPL Microdevices Lab (MDL), and the device was fabricated in the NIST cleanroom.

- ¹P. A. Hiskett, D. Rosenberg, C. G. Peterson, R. J. Hughes, S. Nam, A. E. Lita, A. J. Miller, and J. E. Nordholt, *New J. Phys.* **8**, 193 (2006).
- ²M. D. Eisaman, J. Fan, A. Migdall, and S. V. Polyakov, *Rev. Sci. Instrum.* **82**, 071101 (2011).
- ³E. Knill, R. Laflamme, and G. J. Milburn, *Nature* **409**, 46 (2001).
- ⁴G. N. Gol'Tsman, O. Okunev, G. Chulkova, A. Lipatov, A. Semenov, K. Smirnov, B. Voronov, A. Dzardanov, C. Williams, and R. Sobolewski, *Appl. Phys. Lett.* **79**, 705 (2001).
- ⁵K. D. Irwin, *Appl. Phys. Lett.* **66**, 1998 (1995).
- ⁶A. E. Lita, A. J. Miller, and S. W. Nam, *Opt. Express* **16**, 3032 (2008).
- ⁷P. K. Day, H. G. LeDuc, B. A. Mazin, A. Vayonakis, and J. Zmuidzinas, *Nature* **425**, 817 (2003).
- ⁸B. A. Mazin, *AIP Conf. Proc.* **1185**, 135–142 (2009).
- ⁹K. O'Brien, B. Mazin, S. McHugh, S. Meeker, and B. Bumble, in *IAU Symposium* (2012), vol. 285, pp. 385–388.
- ¹⁰B. A. Mazin, B. Bumble, S. R. Meeker, K. O'Brien, S. McHugh, and E. Langman, *Opt. Express* **20**, 1503 (2012).
- ¹¹J. Zmuidzinas, *Annu. Rev. Condens. Matter Phys.* **3**, 169 (2012).
- ¹²H. G. Leduc, B. Bumble, P. K. Day, B. H. Eom, J. Gao, S. Golwala, B. A. Mazin, S. McHugh, A. Merrill, D. C. Moore *et al.*, *Appl. Phys. Lett.* **97**, 102509 (2010).
- ¹³O. Noroozian, P. Day, B. H. Eom, H. Leduc, and J. Zmuidzinas, *IEEE Trans. Microwave Theory Tech.* **60**, 1235 (2012).
- ¹⁴M. R. Vissers, J. Gao, D. S. Wisbey, D. A. Hite, C. C. Tsuei, A. D. Corcoles, M. Steffen, and D. P. Pappas, *Appl. Phys. Lett.* **97**, 232509 (2010).
- ¹⁵M. Sandberg, M. R. Vissers, J. S. Kline, M. Weides, J. Gao, D. S. Wisbey, and D. P. Pappas, *Appl. Phys. Lett.* **100**, 262605 (2012).
- ¹⁶J. Gao, J. Zmuidzinas, B. A. Mazin, H. G. Leduc, and P. K. Day, *Appl. Phys. Lett.* **90**, 102507 (2007).
- ¹⁷See supplementary material at <http://dx.doi.org/10.1063/1.4756916> for a diagram of the hypothetical non-dissipative states and quasiparticle processes involved in the anomalous electrodynamics of TiN.
- ¹⁸B. Sacépé, C. Chapelier, T. I. Baturina, V. M. Vinokur, M. R. Baklanov, and M. Sanquer, *Phys. Rev. Lett.* **101**, 157006 (2008).
- ¹⁹F. London and H. London, *Proc. R. Soc. A* **149**, 71 (1935).
- ²⁰R. Barends, H. L. Hortensius, T. Zijlstra, J. J. A. Baselmans, S. J. C. Yates, J. R. Gao, and T. M. Klapwijk, *Appl. Phys. Lett.* **92**, 223502 (2008).
- ²¹E. F. C. Driessen, P. C. J. J. Coumou, R. R. Tromp, P. J. de Visser, and T. M. Klapwijk, *Phys. Rev. Lett.* **109**, 107003 (2012).
- ²²R. C. Dynes, V. Narayanamurti, and J. P. Garno, *Phys. Rev. Lett.* **41**, 1509 (1978).
- ²³W. Escoffier, C. Chapelier, N. Hadacek, and J.-C. Villégier, *Phys. Rev. Lett.* **93**, 217005 (2004).
- ²⁴J. Gao, J. Zmuidzinas, B. A. Mazin, P. K. Day, and H. G. Leduc, *Nucl. Instrum. Methods Phys. Res. A* **559**, 585 (2006).
- ²⁵J. Gao, Ph.D. dissertation, Caltech, 2008.
- ²⁶B. Ho Eom, P. K. Day, H. G. Leduc, and J. Zmuidzinas, *Nat. Phys.* **8**, 623 (2012).
- ²⁷M. A. Castellanos-Beltran, K. D. Irwin, G. C. Hilton, L. R. Vale, and K. W. Lehnert, *Nat. Phys.* **4**, 929 (2008).